

# Extension of the integrated HydroKinetic Model to BES RHIC and GSI-FAIR nuclear collision energies

Musfer Adzhymambetov\*

*Bogolyubov Institute for Theoretical Physics, Metrolohichna 14b, 03143 Kyiv, Ukraine*

Yuri Sinyukov†

*Bogolyubov Institute for Theoretical Physics, Metrolohichna 14b, 03143 Kyiv, Ukraine and  
Faculty of Physics, Warsaw University of Technology, 75 Koszykowa street, 00-662, Warsaw, Poland*

(Dated: December 3, 2024)

The work presented is devoted to developing the integrated hydrokinetic approach (iHKM) for relativistic nucleus-nucleus collisions. While the previous cycle of works on this topic focused on ultra-relativistic collisions at the top RHIC and different LHC energies, the current work addresses relativistic collisions at the lower energies, specifically ranging from approximately 1 to 50 GeV per nucleon pair in the center-of-mass colliding system. The formation times for the initial state of dense matter in such collisions can be up to three orders of magnitude longer than those in ultra-relativistic collisions. This reflects a fundamentally different nature and formation process, particularly concerning the possible stages of initial state evolution, including thermalization (which may be only partial at very low collision energies), subsequent hydrodynamic expansion, and the final transition of matter evolution into a hadronic cascade. These stages, which are fully realized in ultra-relativistic reactions, can also occur within the energy range of BES RHIC, albeit with distinct time scales. This publication not only advances the theoretical development of iHKM (referred to, if necessary, as the *extended* version of integrated Hydrokinetic Model, iHKMe), but also provides examples of model applications for calculating observables. A systematic description across a wide range of experimental energies, which is preliminary yet quite satisfactory, for spectra, flow, and femtoscopy, will follow this work.

## I. INTRODUCTION

The goal of relativistic heavy ion experiments, which are continuing for more than thirty years at accelerators/colliders of different generations - from the AGS to the LHC, is to create and study the new forms of strongly interacting matter with extremely high densities and temperatures. The energy density reached in such systems resembles that governing the Early Universe just microseconds after the initial singularity [1]. Such matter can form at some internal stage of the nuclei collision process when the system created becomes almost thermal, while the energy density in an expanding fireball is still very high [2–5].

In the 1950s, the idea to describe the proton-proton and nuclear-nuclear collision processes of multi-particle production in the models of hydrodynamics type appeared. This new tendency, as to compare with S-matrix formalism [6–8], has been started from a pure hydrodynamic model, called now the Landau model, where the simplest prescription for initial and final matter states in the collisions of particles/nuclei [9] have been used. Later, in the 80th, further development of the models goes through the so-called Bjorken model [10] and hydrodynamically inspired parametrizations for the final hydro-collision stage (see, e.g. [11]). The consequent development includes all the stages (currently five, more

details are below) of the evolution of superdense matter created in heavy ion collisions. As to the high energy situation, at the top RHIC and all the LHC energies, the new form of matter - quark-gluon plasma and hadron-resonance gas - manifested itself in the soft physics observables which include hadron and photon yields, spectra, and particle correlations. All these measurements are well described (see review[12] in the integrated HydroKinetic Model - iHKM [13, 14], which we will try to generalize for intermediate and small relativistic energies in this paper.

The intermediate and low relativistic range of collision energy experiments are of special interest. The currently acting ones are associated with the Beam Energy Scan program at RHIC (BES RHIC) and the HADES experiment at the GSI accelerator facility. The nearest planning is the Compressed Baryon Matter (CBM) experiment at the GSI-FAIR. Despite collision processes at the LHC, where the transition between hadron and quark-gluon matters is happening without the phase transition (crossover), at the above-mentioned experiments characterized by large net baryon densities in creating matter, one hopes to search for the thermodynamic line of the phase transition between hadron and quark-gluon matters and also try to discover the critical endpoint [15].

Therefore, this series of experiments on relativistic nucleus-nucleus collisions is the guiding light for the development of effective theoretical models of strongly interacting matter. It is essential to take into account that the new forms of matter arise in the collision processes during only one of the concise stages (which lasts  $10^{-23}$

---

\* adzhymambetov@gmail.com

† sinyukov@bitp.kyiv.ua

–  $10^{-22}$  sec) of ultrafast evolution of the matter, and so a detailed analysis of the properties of its new forms needs the construction of a complete (all-stages) dynamic picture of the collisions.

The objective of this paper is to present an extended integrated hydrokinetic model for the soft physics in all mentioned experiments, covering (all together with already developed iHKM for ultra-relativistic energies) the range from 1 GeV up to 10 TeV energies per nucleon colliding pair in their center of mass, within a unified approach based on the extended integrated HydroKinetic Model - iHKMe. The latter will supplement the iHKM, which is already available for ultra-relativistic energies, to the intermediate and low relativistic collision energies. For each considered energy all the possible stages of nuclei collision processes will be investigated within the same unified description as in the original iHKM. The mentioned stages of the matter evolution during the collision process are: the formation of the initial conditions for the system expansion into a vacuum just after the collision, gradual thermalization of created superdense matter (maybe not complete for quite low collision energies, that can happen without hydro-stage), its consequent hydrodynamic evolution for intermediate energies, the translation of the description of hydrodynamic/or partially thermal medium to particle language – so-called particlization, and, finally, the cascade stage for still interacting already individual particles [16]. So, our approach also includes the possibility that at fairly low energies, not all of these stages (e.g., hydro-stage) will be realized/activated.

The description of the soft physics observables within this unified approach allows one to conclude: at which energies the quark-gluon plasma is created, when the phase transition takes place, and whether the critical endpoint occurs at some collision energy. In addition, from the correlation femtoscopy analysis for baryons, it is planned to extract the most important characteristics of their strong interactions, such as scattering lengths and others.

One of the most serious difficulties in describing a complete set of soft physics observables just combining differently developed stages into a single picture was that one needs to start hydrodynamics as soon as possible - just after colliding nuclei overlap. Otherwise, if one starts hydrodynamic evolution later, say, at typical for strong interactions time-scale around 1 fm/c, either spectra, particle correlation functions, or anisotropic flow will describe the experimental data unsatisfactorily. The reason is that at the standard mentioned starting time for viscous hydro-evolution, neither radial nor anisotropic collective flow at the freeze-out stage develops well to describe data, because of a lack of time for pressure to accelerate enough the created system transversally. Such a logic gives rise to intensive theoretical attempts to explain very early thermalization/hydrodynamization: ADS/CFT correspondence [17–22], Unruh effect [23, 24], three-gluon production, etc. They continued for almost two decades, but have not been successful.

Our idea, and later its full realization, was: to get more intensive flow, both the radial and anisotropic, one does not need the pressure gradient in the created fireball and, so, does not need the early fast thermalization [25]. These flows can be well developed because only the geometrical form of the very initial system, which is essentially finite in nucleus-nucleus collisions and, in addition, has an anisotropic shape in non-central collisions. What is very important - in any case, one needs the system's thermalization sooner or later to describe the data, but not necessarily a fast one. If it happens, say, at 1 fm/c the transverse flow will be present already at this (relatively late) thermalization/ hydrodynamization time because they were developed at the pre-thermal stage, even with quite gradually appearing pressure. The corresponding formalism developed allows one to build the full model of heavy ion collisions that incorporate all stages of heavy ion collision processes without the physically controversial hypothesis of the very early system's thermalization [16, 25].

This paper is developing the iHKM model for the intermediate energy range of relativistic nucleus-nucleus collisions: programs BES at RHIC, and future CBM in GSI-FAIR experiments, including current HADES activity. We will call the corresponding new extension of the model in this paper - iHKMe, or again iHKM when it is clear for which energy it is applied. The main modification in the newly developed model concerns the formation of initial conditions of matter evolution in relativistic A+A collisions at relatively small energies. In already built iHKM the overlapping time of colliding nuclei is around  $10^{-3}$  fm/c at the energy 5.02 ATeV. At BES RHIC energy, e.g., 14.5 AGeV it is 1.6 fm/c.

It is clear, that the model of initial conditions for the consequent pre-thermal (thermalization) stage are very different. While in iHKM we use a hybrid approach based on MC-GLAUBER calculations, realized in the GLISSANDO-2 model [26] in the transverse direction, and Color Glass Condensate in the longitudinal one, the initial conditions are dramatically changed in the collisions at BES RHIC and below energies where the overlapping time is differed (larger) by 3 order of the value. The initial conditions in the extended for intermediate and small relativistic heavy ion collision energies model - iHKMe are based on the quasiclassical UrQMD simulations [27] with added quantum (and classical) fluctuations during the thermalization process. It leads to partial thermal evolution of the matter, created at small and intermediate collision energies.

The goal of this paper is to propose the theoretical basis for the description of the soft physics at the intermediate and small relativistic energies, in addition to what has been done already for ultrarelativistic energies (iHKM), and also illustrate the results of the developed model at one of the collision energies. A consistent description of the observables within iHKMe/iHKM in BES RHIC and GSI-FAIR experiments will be presented in subsequent publications.

## II. MODEL DESCRIPTION

### A. The basic aspects of the approach

In the extended version of iHKM - we call it iHKMe - we rely on the transport UrQMD model for the very initial pre-equilibrium dynamics at low and intermediate relativistic collision energies. The possibility to use for the same aim in other similar models like SMASH [28] is planned in future publications.

The problem of transformation of the hydrodynamic approach to particle evolution language and vice-versa is quite non-trivial. Especially if it concerns the low enough but still relativistic energies, e.g., at  $\sqrt{s} < 10A$  GeV for  $A + A$  collisions. The reasons for this are the following.

First, the obvious problem is that during UrQMD (or SMASH) simulations of the initial stage of collisions, the gradual transformation, at least of part of the total system, to a hydrodynamic subsystem cannot be based on the initial singular distribution of particles in one cascade event. So, one needs to use some kind of smoothing/averaging even for event-by-event analysis.

Second, the system may not be hydrodynamized completely at very low energies. The hydrodynamically expanding part of the matter transforms to final particles just into the surrounding part of the interacting hadron gas which escaped the hydrodynamic phase during the total matter evolution. The process of transition of hydrodynamically expanding part of the matter into hadrons is called particlization and is the starting point for the consequent stage of hadron cascade evolution. In this picture, the main theoretical point is the explanation of the real physical mechanism of thermalization/hydrodynamization. The approach [16] which we use now, is phenomenologically described by utilizing the thermalization and relaxation times within the Boltzmann equation approximation. The gradual transformation of the initially non-thermal matter into (partially) thermalized matter is governed by conservation law equations.

Third, the important question concerns the nature of the thermal fluid that appears against the backdrop of the initial UrQMD (or SMASH) gas of colliding hadrons. We suppose that initially, it appears due to local quantum and classical density fluctuations through the QCD droplet formation. Similar to our first point (see above) even at event-by-event analysis the smoothing procedure is necessary to describe some stage of the collision process in continuous medium approximation. We just smooth out the droplet picture for very high-density local fluctuations into an effectively hydrodynamic one.

Fourth, the question appears about the particlization of the fluid component. At not very low relativistic energies, at some stage of the matter evolution, the droplets (even without any smearing) can merge into liquid and this substance fills almost the entire system. Then the description of the particlization process has a standard form *a la* Cooper-Frey prescription. However, at low en-

ergies, density fluctuations that form droplets may be rare and, accordingly, the corresponding hydrodynamically averaged component is small (or even absent), and a significant part of the system consists of the UrQMD-particle component at the hypersurface of particlization. This possible scenario should also be developed in the iHKMe approach, designed to describe nuclear collisions at energies from 1-3 to 40-50 AGeV.

Let us consider the particlization and its condition in some detail. We start with a pure hydrodynamic system. A near-local thermal equilibrium and hydrodynamic behavior can be maintained in a finite expanding system as long as the collision rate among the particles is much faster than the expansion rate. Since densities drop out during 3-dim expansion intensively, the collision rate decreases rapidly and the system eventually falls out of equilibrium. As a result, the hydrodynamic medium decouples and freeze-out or the hadron cascade phase happens.

The inverse expansion rate is the collective expansion time scale [29]:

$$\tau_{\text{exp}} = - \left( \frac{1}{n} \frac{\partial n}{\partial t^*} \right)^{-1} = - \left( \frac{1}{n} u^\mu \partial_\mu n \right)^{-1} = \frac{1}{\partial_\mu u^\mu}, \quad (1)$$

where  $t^*$  is the proper time in the fluid's local rest system. The last approximate equality follows from the conservation of particle number density currents at the last stage of the hydro-expansion.

The inverse scattering rate of particle species  $i$  is the mean time between scattering events for particle  $i$ ,  $\tau_{\text{scat}}^{(i)}$ :

$$\tau_{\text{scat}}^{(i)} \approx \frac{1}{\sum \langle v_{ij} \sigma_{ij} \rangle n_j}, \quad (2)$$

where  $v_{ij}$  is the relative velocity between the scattering particles and  $\sigma_{ij}$  is the total cross section between particles  $i$  and  $j$ , the sharp brackets mean an average over the local thermal distributions. This time is determined by the densities of all particles with which particle  $i$  can scatter, and the corresponding scattering cross sections. Let us estimate the mean time between scatterings for pions,  $\tau_{\text{scat}}^{(\pi)}$ . First, note that  $\tau_{\text{scat}}^{(i)} > \lambda^{(i)}$ , where  $\lambda^{(i)}$  is mean free path for particle species  $i$ :

$$\lambda^{(i)} \approx \frac{1}{\sum \langle \sigma_{ij} \rangle n_j}, \quad (3)$$

so  $\lambda_{\text{scat}}^{(i)}$  represents the lower limit for  $\tau_{\text{scat}}^{(i)}$ . For example, the pion mean free path in the rest frame of the fluid element at freeze-out,  $\lambda^{(\pi)}(\tau_{f.o.})$ , was roughly estimated as the following [29]

$$\lambda^{(\pi)}(\tau_{f.o.}) \approx \frac{1}{\sigma_{\pi p} n_B + \sigma_{\pi\pi} n_M} \quad (4)$$

with the parameters  $\sigma_{\pi p} = 65$  mb to be total cross section for pion-proton scattering, and the same cross-section for all non-strange baryons, whereas  $\sigma_{\pi\pi} = 10$

mb is the total cross-section for pion-pion scattering and the same cross-section for all non-strange mesons.

In the above approximation for fluid decoupling, the following equations should be satisfied

$$\tau_{scat}(T(x), \mu(x)) = \tau_{exp}(T(x), \mu(x)) \quad (5)$$

where  $T(x)$  and  $\mu_B(x)$  are the local temperature and baryonic chemical potential correspondingly. It is a complicated but promising way to build the true-like decay hypersurface for near-local equilibrium *baryon-reach* expanding matter.

Another criterium that is based on the energy densities in fluid, can be

$$\epsilon(T(x), \mu_B(x)) = \epsilon_{dec} = const. \quad (6)$$

However, there is only hope that there exists some parameter  $\epsilon_{dec}$  when the criteria (5) and (6) will near coincide. In this paper, we will follow more simple criteria of decoupling based on the energy density (6).

The realistic situation, however, can be more complicated, even at the selected criteria: in the case of low collision energies, the system may never reach a complete thermalization, only, if possible, a partial one. In such a case, in spite of near full thermalization at the particlization stage at high enough energies, the system at the decaying (into the interacting particles) stage consists of two expanding components of baryon reach matter: UrQMD gas and fluid. The most natural way then is to select the energy density interval when the mechanism, forming the dense (QGP?) droplets stops working and soon after the corresponding (see above) hydrodynamical part of the system decays into hadrons without reaching the full thermalization. In our approximation, it means that one has to transform the hydrodynamically involved part of the system into particles at this droplet's (mean) decaying time. So, because we do not know the quantum component of the QCD fluctuations, the corresponding energy density, at which the decay of the hydro-component at small relativistic energies happens, is a free parameter. The corresponding particle injection from this decay of hydro-component in the case of not full thermalization is just added to the preserved yet UrQMD component. Of course, the local energy-momentum conservation law for the evolution and hydro-decays of the total system, consisting of both UrQMD (or SMASH) and hydro-components, must be implemented in any scenario. It is done in the iHKMe (like in iHKM) scenario that is developed in the presented article.

However, as we already marked, switching from quasiclassical microscopic models (UrQMD, SMASH, etc...) to the macroscopic hydrodynamic regime could be impossible if one naively tries to based on a distribution function from a single transport simulation, it brings significant fluctuations in coordinates and anisotropies in momentum space, contradicting the basic assumptions of hydrodynamics. So, one needs to use some averaging procedure to provide smooth initial conditions for a con-

sequent description of hydrodynamic expansion and, of course, especially, for event-by-event analysis.

There are two common solutions to this problem. The straightforward one is to generate huge amounts of events and then average over them. However, to study the influence of fluctuations in the initial conditions on the final observables one needs to introduce some similarity criteria between events. Of course, averaging over the centrality class might be too rough and unsuitable for event-by-event analysis. The common approach to this problem is applying some Gaussian smearing procedure to each particle and then constructing only the time component of the stress-energy tensor  $T^{0\mu}$  and baryon current  $J_\mu^0$ . The other components are restored using an equation of state and explicit representation of the relativistic hydrodynamic tensors through macroscopic fields of velocity  $u^\mu$ , energy-density  $\epsilon$ , pressure  $p$ , and baryon density  $n_B$ .

In the paper [30], a comparison of such a procedure across several hybrid models is presented. Additionally, the same paper introduces a Lorentz-invariant Gaussian kernel for particle smearing over the space but at constant time  $t$  (See also [31])

$$\mathcal{K}(\mathbf{r}) = \frac{\gamma}{(2\pi\sigma^2)^{3/2}} \exp\left(\frac{-\mathbf{r}^2 - (\mathbf{r} \cdot \mathbf{u})^2}{2\sigma^2}\right), \quad (7)$$

where  $\mathbf{u}$  is velocity of the particle and  $\gamma$  is the Lorentz contraction factor. Such a procedure can be attributed to the averaging over an ensemble of "similar" collision events without generating them. The similarity between the events is described by the  $\sigma$  parameter.

In this paper, we propose a modification of this kernel for particle smearing on an arbitrary hypersurface  $\sigma^\mu$ . For a particle  $i$  with baryon charge  $B_i$ , momentum  $p_i^\mu$ , velocity  $u_i^\mu = p_i^\mu/p_i^0$ , and space position  $x_i^\mu$ , the relative contribution of its energy, momentum, and charges to the lattice grid cell  $\Delta\sigma_j^\mu$  with the center at  $x_j^\mu$  and normal vector  $n_j^\mu$  is given by

$$\mathcal{K}_{ij} = \frac{n_j^\lambda u_{i\lambda}}{(\pi R^2)^{3/2}} \exp\left(\frac{r_{ij}^\mu (g_{\mu\nu} - u_\mu^i u_\nu^i) r_{ij}^\nu}{R^2}\right). \quad (8)$$

Here,  $r_{ij}^\mu = x_i^\mu - x_j^\mu$  represents the radius vector between the particle and the center of the cell ( $x_i, x_j \in \sigma^\mu$ ), while  $R$  is a free scalar parameter. We utilize the kernel (8) on hypersurfaces of constant proper time  $\tau = const$ . Then, for a cell with space-rapidity  $\eta_j$ ,

$$\Delta\sigma^\mu = n^\mu \Delta x \Delta y \Delta \eta, \quad (9)$$

$$n^\mu = (\tau \cosh \eta, 0, 0, \tau \sinh \eta), \quad (10)$$

where  $\Delta x, \Delta y, \Delta \eta$  are cell sizes in three directions, with the numerical values 0.3 fm, 0.3 fm, and 0.05 respectively.

Utilizing kernel (8) we obtain the following inputs for

the next stages of the model:

$$T_{\text{urqmd}}^{\mu\nu}(\tau; x_j) = \sum_i \frac{p_i^\mu p_i^\nu}{p_i^0} \mathcal{K}_{ij}, \quad (11)$$

$$J_{\text{urqmd}}^\mu(\tau; x_j) = \sum_i B_i \frac{p_i^\mu}{p_i^0} \mathcal{K}_{ij}, \quad (12)$$

where sums are taken over all the particles from UrQMD evolution which satisfy the condition

$$\left| \sqrt{t_i^2 - z_i^2} - \tau \right| < \Delta\tau/2. \quad (13)$$

Notice that the pre-equilibrium UrQMD evolution is conducted in Cartesian coordinates  $(t, x, y, z)$  with the time step  $\Delta t = \Delta\tau$ . We verified that the selection of particles with Eq. (13) yields fluctuations of conserving charges which do not exceed 2%. On the other hand, violations of the normalization relation,  $\sum_j K_{ij} = 1$ , due to the discreteness of the lattice cells result in a deviation for conserving changes of only 0.5%.

Lastly, let us note that in this paper we do not consider separate equations for electric charge and strangeness assuming locally  $n_s = 0$  and  $n_q = A/Zn_B \approx 0.4n_B$  for gold nuclei.

## B. Thermalization

One of the key aspects of iHKM is the thermalization stage, in other words, the hydrodynamization process. During this stage, matter can be phenomenologically split into two distinct components: a (near) local equilibrium one, described by macroscopic fields, and non-thermalized components represented by out-of-equilibrium hadrons and strings evolving via UrQMD. These components contribute to the non-equilibrium energy-momentum tensor [13] and the charge currents, so that the corresponding equations guarantee the conservation laws of the corresponding values for the total systems.

$$T_{\text{total}}^{\mu\nu}(x) = T_{\text{urqmd}}^{\mu\nu}(x) \cdot \mathcal{P}_\tau + T_{\text{hydro}}^{\mu\nu}(x) \cdot (1 - \mathcal{P}_\tau), \quad (14)$$

$$J_{\text{total}}^\mu(x) = J_{\text{urqmd}}^\mu(x) \cdot \mathcal{P}_\tau + J_{\text{hydro}}^\mu(x) \cdot (1 - \mathcal{P}_\tau), \quad (15)$$

where  $\mathcal{P}_\tau = \mathcal{P}(\tau)$  is a weight function such that  $\mathcal{P}(\tau_0) = 1$  at the start of the thermalization stage,  $\mathcal{P}(\tau_{th}) = 0$  at the end, and  $0 < \mathcal{P}(\tau_0 < \tau < \tau_{th}) < 1$  in between. Its explicit form will be discussed later. Both total stress-energy tensor and baryon current obey conservation laws:

$$\partial_\mu T_{\text{total}}^{\mu\nu}(x) = 0; \quad \partial_\mu J_{\text{total}}^\mu(x) = 0. \quad (16)$$

Exploiting the conservation laws accounted for in UrQMD evolution

$$\partial_\mu T_{\text{urqmd}}^{\mu\nu}(x) = 0, \quad \partial_\mu J_{\text{urqmd}}^\mu(x) = 0 \quad (17)$$

we obtain hydrodynamic-like equations with a source for re-scaled tensors

$$\partial_\mu \tilde{T}_{\text{hydro}}^{\mu\nu}(x) = -T_{\text{urqmd}}^{\mu\nu}(x) \cdot \partial_\mu \mathcal{P}_\tau, \quad (18)$$

$$\partial_\mu \tilde{J}_{\text{hydro}}^\mu(x) = -J_{\text{urqmd}}^\mu(x) \cdot \partial_\mu \mathcal{P}_\tau. \quad (19)$$

Here the re-scaled (tilded) hydrodynamic tensors are defined as

$$\tilde{T}_{\text{hydro}}^{\mu\nu}(x) = T_{\text{hydro}}^{\mu\nu}(x) \cdot (1 - \mathcal{P}_\tau), \quad (20)$$

$$\tilde{J}_{\text{hydro}}^\mu(x) = J_{\text{hydro}}^\mu(x) \cdot (1 - \mathcal{P}_\tau), \quad (21)$$

As the previous papers [13, 32], we utilize the same ansatz inspired by the Boltzmann equation in relaxation time approximation, with probability  $\mathcal{P}(\tau)$

$$\mathcal{P}(\tau) = \left( \frac{\tau_{th} - \tau}{\tau_{th} - \tau_0} \right)^{\frac{\tau_{th} - \tau_0}{\tau_{rel}}}. \quad (22)$$

Wherein a free parameter of the model  $0 < \tau_{rel} < \tau_{th} - \tau_0$  is introduced. The relaxation time  $\tau_{rel}$  characterizes the rate of the thermalization process. To avoid introducing additional freedom during the model calibration, in this paper, we set the relaxation time at its minimum value  $\tau_{rel} = \tau_{th} - \tau_0$ . At the same time, the influence of non-thermal dynamics can be varied via the thermalization time  $\tau_{th}$ .

Solving Eqs. (18) and (19) constitutes the primary objective of the relaxation stage in the model. These equations are employed to update, over time  $\tau$ , the values of the time components of the corresponding tensors  $\tilde{T}_{\text{hydro}}^{0\mu}$  and  $\tilde{J}_{\text{hydro}}^0$  for each cell of the spatial grid. The remaining components are restored using the Israel-Stewart form [33] of the tensors:

$$\frac{\tilde{T}_{\text{hydro}}^{\mu\nu}}{1 - \mathcal{P}_\tau} = T_{\text{hydro}}^{\mu\nu}(x) = (\epsilon + p) u^\mu u^\nu - pg^{\mu\nu} + \pi^{\mu\nu}. \quad (23)$$

$$\frac{\tilde{J}_{\text{hydro}}^\mu}{1 - \mathcal{P}_\tau} = J_{\text{hydro}}^\mu(x) = n_B u^\mu, \quad (24)$$

where  $\epsilon$ ,  $p$ , and  $n_B$  represent the local energy density, pressure, and baryonic density, respectively.  $u^\mu$  denotes the four-velocity of the fluid,  $g^{\mu\nu}$  is the metric tensor, and  $\pi^{\mu\nu}$  stands for the shear-stress tensor. The local energy density, pressure, and four-velocity are derived from  $T_{\text{hydro}}^{0\mu}$  utilizing the equation of state  $p = p(\epsilon, n_B)$ . At the same time, the shear-stress tensor evolves according to an independent equation within the Israel-Stewart framework [16, 33]. To numerically solve Eqs. (18) and (19), we utilize the vHLL code [34] with modifications adjusting source terms [16]. We do not consider other transport coefficients, such as bulk pressure, diffusion, and heat conductivity in this paper. We employ two different equations of state, namely the chiral EOS [35] with a crossover-type transition between QGP and the hadron stages and the AZHYDRO EOS with a first-order phase transition proposed in [36].

### C. Hydrodynamic expansion

We suppose, that not only at ultrarelativistic heavy ion collisions but also, at least, at intermediate energies at BES RHIC, at some  $\tau = \tau_{th}$  the system attains a state of local near-equilibrium, characterized by hydrodynamic tensors  $T_{\text{total}}^{\mu\nu} = T_{\text{hydro}}^{\mu\nu}$  and  $J_{\text{total}}^{\mu} = J_{\text{hydro}}^{\mu}$ , with the source terms in Eqs. (20) and (21) vanishing. Below we will discuss the more complicated situation. In simple cases the hydrodynamic evolution persists until the system becomes dilute and departs from partial local equilibrium, which means that hydrodynamic approximation destroys and particle language is necessary. Then the system is appropriately described in microscopic terms using a hadron-resonance gas model, UrQMD in the case of this study.

The anticipated outcome of the hydrodynamic stage is the formation of a hypersurface that marks the transition between the fluid and gas phases, often referred to as the 'particlization hypersurface', and denoted as  $\sigma_{sw}$  in this paper. As we wrote before, We carry out this transition at a fixed energy density  $\epsilon_{sw}$  for simplicity. In our model, the construction of the particlization hypersurface is achieved using the Cornelius routine [37, 38].

When dealing with low-energy collisions at  $\sqrt{s_{NN}} \sim 3 - 10$  GeV, as observed in experiments such as HADES, RHIC BES, or CBM, it is reasonable to anticipate that the system may not achieve complete thermalization. Consequently, extending the particlization hypersurface criteria  $\sigma_{sw}$  into the thermalization phase,  $\tau < \tau_{th}$ , becomes imperative.

During the thermalization period, it is noteworthy that there exist three distinct ways to define energy density:

1. The local equilibrium energy density  $\epsilon_{\text{hydro}}$ , derived from  $T_{\text{hydro}}^{\mu\nu}$ .
2. The non-equilibrium energy density  $\epsilon_{\text{urqmd}}$  derived from  $T_{\text{urqmd}}^{\mu\nu}$ .
3. The mixed energy density  $\epsilon_{\text{total}}$  derived from the total energy-momentum tensor  $T_{\text{total}}^{\mu\nu}$ .

While it is conventional to associate the particlization hypersurface with the total energy density of the system, we opt to utilize  $\epsilon_{\text{hydro}}$  instead. The matter may not be fully thermalized at quite small collision energies, so  $\mathcal{P}$  becomes a free parameter instead of  $\tau_{th}$ . So, at such energies, it is possible that hydrodynamics just inject thermal particles into expanding (and still existing!) UrQMD-system. Then the totally non-locally equilibrated system will include injecting initially (locally) thermal particles from hydrodynamics. The latter can be easily calculated by using a generalized Cooper-Frye prescription with collective velocities  $u^{\mu}$  of the pure hydrodynamical part accounting for a known equation of state. It is notably simpler and faster than utilization for building the decay hypersurface for the total momentum-energy tensor. Notice, in addition, that the criteria described in subsection II A apply to locally equilibrated systems but not to

mixtures of equilibrated and non-equilibrated systems. The proposed method addresses several technical challenges simultaneously.

A few technical details. Minor time fluctuations can emerge in UrQMD tensors due to the transition from Cartesian to Milne coordinates during the thermalization stage as in Eq. (13). They disappear if we average over several time steps. Consequently, as Eq. (18) implies, a smooth transition from the source to hydrodynamic tensors occurs. After several time steps, the hydrodynamic component behaves regularly over time, providing a smooth particlization hypersurface.

### D. Particlization

Following the transition through the particlization hypersurface, the matter becomes sufficiently dilute to be effectively described as a hadron-resonance gas. In the iHKMe, the injection of hadrons occurs from two distinct sources: equilibrium (eq) and non-equilibrium (n.eq)

$$N_{\text{total}} = N_{\text{eq}} + N_{\text{n.eq}}. \quad (25)$$

The particles from both components are injected into the afterburner cascade locally on the particlization hypersurface  $\sigma_{sw}$  from the corresponding distribution function.

#### 1. Emission of thermal particles

The emission from the near-equilibrium source can be characterized using the well-established Cooper-Frye procedure [39] with small modifications discussed later. In this prescription, the yield of hadrons of the species  $i$  is given by:

$$N_{\text{eq}}^i = \int d^3p \int \frac{d\sigma_{\mu} p^{\mu}}{p_0} (1 - \mathcal{P}(\tau)) f_i(x, p), \quad (26)$$

where  $d\sigma_{\mu}$  is a small part of the hypersurface  $\sigma_{sw}$ , and  $f_i$  is the near-equilibrium distribution function. Notice here the additional  $1 - \mathcal{P}(\tau)$  factor which is not equal to one during the relaxation stage.

The distribution function  $f_i(x, p)$  depends on the local thermodynamic properties of the system, temperature, chemical potential, and shear stress tensor. The velocity of the fluid  $u_{\mu}$ , the shear-stress tensor  $\pi^{\mu\nu}(x)$ , and the baryon charge density  $n_B$  are extracted from the hydrodynamics energy-momentum tensor and baryon current. The baryon, electric, and strange chemical potentials, as well as the temperature, are obtained from the energy density  $\epsilon$  and the charge densities  $n_b, n_q = 0.4n_b, n_s = 0$ , using the equation of state. The chemical potential  $\mu_i$  for each particle species can then be determined from the following relation:

### 3. Non-space-like surface emission treatment

$$\mu_i = B_i \mu_B + q_i \mu_q + s_i \mu_s, \quad (27)$$

where  $B_i$ ,  $q_i$ , and  $s_i$  represent the particle's baryon, electric, and strange charges, respectively. The near-equilibrium distribution functions  $f_i(x, p)$  are obtained after applying the Grad ansatz [40] for viscous corrections to the corresponding local equilibrium distribution functions  $f_i^{eq}(x, p)$ . Assuming the same corrections for all hadron species, the thermal particle production can be written as:

$$\frac{d^3 N_i}{dp d(\cos \theta) d\phi} = (1 - \mathcal{P}_\tau) \frac{d\sigma_\mu p^\mu}{p_0} p^2 f_{eq}(p^0, T, \mu_i) \times \left( 1 + (1 \mp f_{eq}) \frac{p_\mu p_\nu \pi^{*\mu\nu}}{2T^2(\epsilon + p)} \right), \quad (28)$$

Here, the asterisk denotes the local rest frame of the fluid element, and  $\mp$  indicates Fermi/Bose statistics. For more detailed information, we refer the reader to the papers [13] or [41].

### 2. Non-thermal emission

The non-equilibrium component is emitted in a similar fashion.

$$N_{n,eq}^i = \int d^3 p \int \frac{d\sigma_\mu p^\mu}{p_0} \mathcal{P}(\tau) f_i^{n,eq}(x, p). \quad (29)$$

However instead of generating particles from the distribution function  $f_i^{n,eq}(x, p)$  we utilize the particles from the sub-ensemble constructed during the pre-equilibrium dynamics stage regarding non-thermal emission. Then, for each piece of the particlization hypersurface  $d\sigma_j^\mu$  located at  $x_j^\mu$ , the probability that a particle with space-time position  $x_i^\mu$  will be emitted is defined by the product:

$$\mathcal{G}(p_i, x_i; d\sigma_j) = \theta(p_i^\mu d\sigma_j^\mu) \times \theta\left(\frac{\Delta\tau}{2} - |\tau_j - \tau_i|\right) \times \mathcal{K}_{ij} \times \frac{p_i^\mu d\sigma_j^\mu}{p_i^0}. \quad (30)$$

The first Heaviside step ensures that particles fly from the hotter to the colder phase. The following two multipliers come from the construction of the nonequilibrium distribution function in Eqs. (8) and (13). These terms determine whether the particle intersects the hypersurface in space and time. The last term is related to the size and space-time orientation of the hypersurface. Summing over all hypersurface and all particle tracks with the  $\mathcal{P}_\tau$  weight yields the total contribution of non-thermal emission.

$$N_{n,eq} = \sum_{i \in \{tracks\}} \sum_{j \in \{\sigma_{sw}\}} \mathcal{P}_{\tau_j} \mathcal{G}(p_i, x_i; d\sigma_j). \quad (31)$$

It is well-known that the hypersurface of constant energy density might include problematic regions [42] 'sink' terms with  $d\sigma_0 < 0$  and non-space-like parts, with by  $d\sigma^\mu d\sigma_\mu < 0$ . In both cases, not all particles near the surface can cross it  $p^\mu d\sigma_\mu < 0$  leading to negative contributions in the Cooper-Frye formula (26).

To address this problem adequately, we adopt a prescription proposed in [42, 43], which suggests substituting  $p^\mu$  with a generalized momentum  $\pi^\mu$  in the near-equilibrium distribution function in Eq. (28).

$$\pi^\mu(x, p) = p^\mu \theta(1 - \lambda) + u^\mu (p \cdot u) \theta(\lambda - 1), \quad (32)$$

where  $\theta$  is the Heaviside step function and  $\lambda$  is defined by:

$$\lambda = \lambda(x, p) = \left| 1 - \frac{p \cdot n}{(p \cdot u)(n \cdot u)} \right|. \quad (33)$$

In this formula,  $n^\mu$  represents the normal vector to  $d\sigma$ . This substitution modifies the distribution function in a manner that preserves the number of emitted particles but slightly violates energy conservation. We refer the reader to the paper [43] for a more detailed explanation.

### E. Hadronic cascade

At the final post-hydrodynamical stage of the system's evolution, all particles from both equilibrium and non-equilibrium sources are input into the UrQMD hadron cascade code [27]. In the iHKM framework, we aim to account for all reliably known hadron resonance states, even those not processed by UrQMD. Therefore, heavy resonances not present in the UrQMD particle database are decayed right at  $\sigma_{sw}$  to ensure energy-momentum conservation.

We generate 20 to 200 UrQMD events based on a single hydrodynamic run to increase statistics in event-by-event simulation. A detailed discussion of this procedure can be found in [44]. It's worth noting that this approach saves CPU time while, as demonstrated in similar models such as [41] and the iHKM analysis, it does not significantly impact the final observables, including Bose-Einstein correlations. However, we expect that artificial correlations might be present at several GeV energies when the multiplicities of thermal particles are relatively low due to this procedure. Therefore, it is reasonable to stick with a pure event-by-event simulation. However, this should not be the case for the 14.5 GeV energies considered in all the simulation results presented in this paper.

### III. MODEL CALIBRATION AND RESULTS

For demonstration purposes in this paper, we focus exclusively on Au+Au collisions at  $\sqrt{s_{NN}} = 14.5$  GeV within the RHIC BES program. This experiment is an intermediate point between the lower-energy collisions at several GeV and the higher-energy collisions reaching several tens of GeV.

#### A. Smoothing procedure

To perform hydrodynamics simulations, starting with a smooth initial distribution of thermalized matter is necessary. However, capturing event-to-event fluctuations in the system's initial state is essential for reproducing experimental data accurately. Models that rely on a transport approach to carry out pre-thermal dynamics usually derive the distribution function from a single event by applying Gaussian smearing to point-like particles with a kernel similar to Eq.(7) or Eq.(8), introducing free parameters to the model [45–48].

One of the peculiarities of the iHKM is the presence of a continuous thermalization stage, which additionally smooths out the distribution of matter. In Figure 1 we demonstrate the energy density distribution in the transverse plane at zero space rapidity  $\eta$  in scenarios with and without the thermalization stage at the same time  $\tau_{th}$ . This noticeable difference can significantly influence the final observables and consequently our estimation of the model's optimal parameters, including the equation of state and transport coefficients.

#### B. Free parameters and calibration

Let us briefly summarize the free parameters of the model. They can be categorized into three groups:

1. Responsible for thermalization stage:
  - $\tau_0$  - start of thermalization stage
  - $\tau_{rel}$  - relaxation time
  - $\tau_{th}$  - end of thermalization stage
2. Smoothing parameter  $R$
3. Thermodynamical properties
  - equation of state
  - transport coefficients, e.g.  $\eta/s$
  - particlization energy density  $\epsilon_{sw}$

To calibrate  $\tau_0$  and  $\tau_{th}$  we utilize experimental data for  $\pi^-$  transverse momentum spectra varying values of these parameters around the typical scale of

$$\tau_{\text{overlap}} = \frac{2R_N}{\sqrt{(\sqrt{s_{NN}}/2m_N)^2 - 1}}, \quad (34)$$

It represents the time required for two nuclei to overlap completely as they move with their initial rapidities. In this equation,  $R_N$  stands for the radius of one nucleus, and  $m_N$  stands for the nucleon mass. To simplify the model calibration, reduce the number of free parameters, and save CPU time we use a simple ansatz for the relaxation time fixing it a maximum allowed value as:

$$\tau_{rel} = \tau_{th} - \tau_0.$$

To determine the shear viscosity  $\eta/s$ , we start from the typical minimal value of  $1/4\pi$  [49] and increase it if the flow anisotropy  $v_2$  is too strong in non-central collisions compared to the experimental data.

For the transition to the afterburner stage, we use a typical value for the energy density  $\epsilon_{sw} = 0.5$  GeV/c, which lies in the range where the equations of state for the liquid and gas phases of strongly interacting matter coincide. However, reducing this value might enhance the results due to the less intense hadron annihilation process in UrQMD compared to local-equilibrium hydrodynamics. Specifically, we observe the sensitivity of  $\bar{p}/p$  to  $\epsilon_{sw}$ , prompting us to treat  $\epsilon_{sw}$  as a free parameter if necessary. The final sets of parameters we employed to simulate Au+Au collisions at  $\sqrt{s_{NN}} = 14.5$  GeV with two different equations of state are presented in Table I.

#### C. Bulk observables

This section presents our results using the tuned set of free parameters. The transverse momentum spectra for the lightest hadrons production in 0 – 5% and 20 – 30% centrality classes are shown in Fig. 2. It is evident that the model underestimates the  $\bar{p}/p$  ratio, particularly noticeable in central collisions, and adjusting the free parameters does not fully resolve this discrepancy. This issue might be mitigated by considering dissipative terms in the baryon current (24), which could reduce the baryon chemical potential within the midrapidity region of the system. However, it could also indicate an overestimation of baryon stopping in the UrQMD model in combination with the hydrodynamization in the intermediate collision energy regime.

TABLE I. Parameters of iHKM providing the best description of bulk observables for Au+Au collisions at  $\sqrt{s_{NN}} = 14.5$  GeV.

| Title | EoS                 | $R$    | $\tau_0$ | $\tau_{th}$ | $\eta/s$ | $\epsilon_{sw}$          |
|-------|---------------------|--------|----------|-------------|----------|--------------------------|
| set 1 | Chiral <sup>a</sup> | 0.5 fm | 1.2 fm/c | 2.6 fm/c    | 0.08     | 0.5 GeV/fm <sup>3</sup>  |
| set 2 | PT1 <sup>b</sup>    | 0.5 fm | 1.4 fm/c | 1.8 fm/c    | 0.08     | 0.35 GeV/fm <sup>3</sup> |

<sup>a</sup> EoS with crossover transition from [35].

<sup>b</sup> EoS with first-order phase transition from [36].



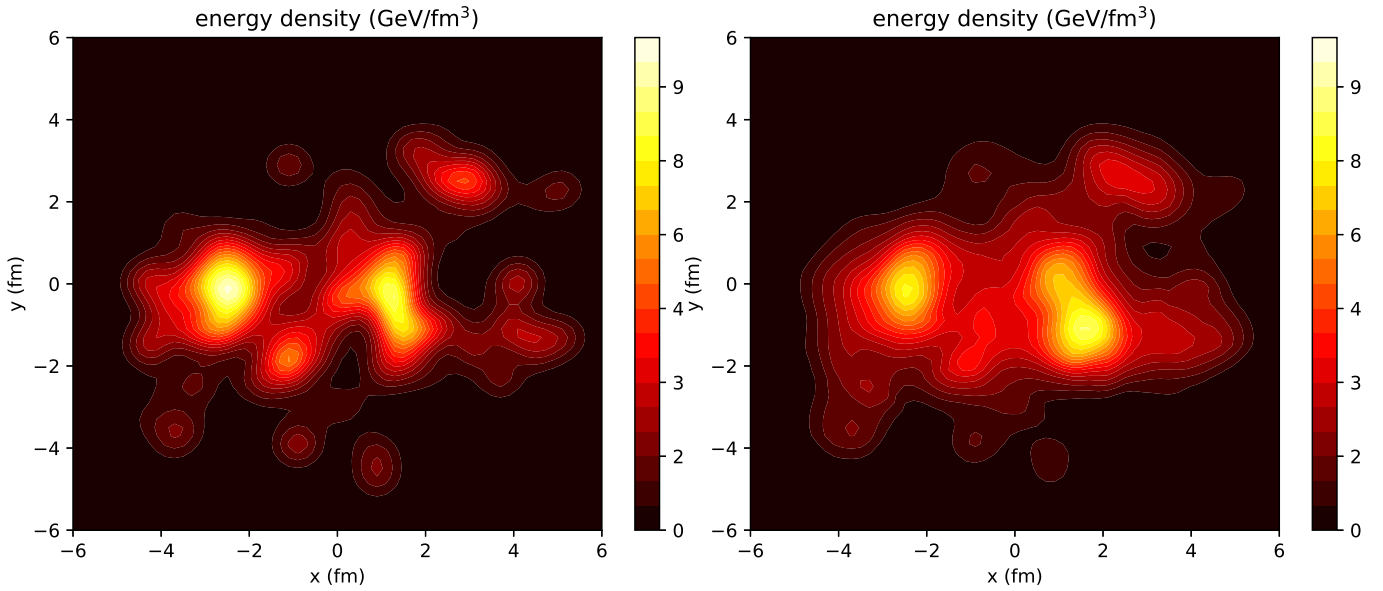


FIG. 1. Energy density distribution in the transverse plane at  $z = 0$  (i.e. zero space rapidity  $\eta = 0$ ). The same event of Au+Au collisions at  $\sqrt{s_{NN}} = 14.5$  GeV from 20-30% centrality class. Left: energy density extracted from the UrQMD tensor (14) at  $\tau = \tau_{th} = 2.6$  fm/c. Right: energy density in iHKM simulations at the same proper time  $\tau_{th}$ .

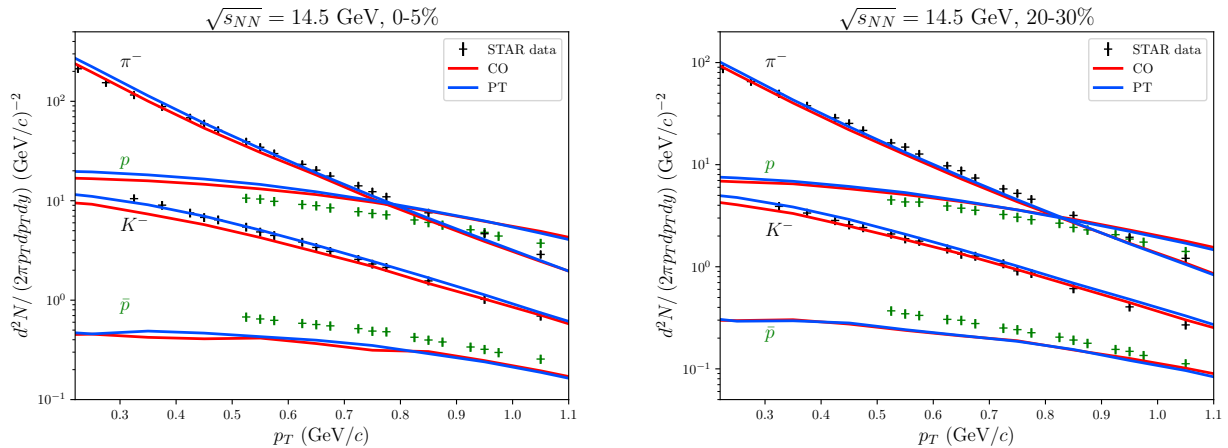


FIG. 2. Transverse momentum spectra of (anti-) protons, and negatively charged kaons and pions from 0-5% (left) and 20-30% (right) centrality classes. iHKM parameters are described in Table I. STAR data is taken from [50].

We also compare iHKM results for  $p_T$  dependence of the elliptic flow obtained via  $\eta$ -subtraction method  $v_2\{\eta - \text{Sub}\}$ . Three centralities presented in STAR collaboration paper [50] are considered. In Fig. 3 one can see that the chiral EoS (Set 1) results are very close to the data. Meanwhile, iHKM calculations with a phase transition (Set 2) struggle to reach the experimental value of the flow in non-central collisions even at low share viscosity to entropy ratio  $\eta/s = 0.08$ . Further viscosity reduction improves only the high- $p_T$  behavior ( $p_T > 1$  GeV/c) while dramatically worsening the spectra. The model results for  $v_2$  could be improved by decreasing thermalization time  $\tau_{th}$ , but too fast thermalization seems unrealistic. Another possibility to improve results is to treat  $\tau_0$

and  $\tau_{th}$  as free parameters for different centrality classes. However, this is out of the scope of this paper.

Lastly, we present our two-pion interferometry results for 5% most central collisions. Particle selection was done according to STAR acceptance [51]:  $|y| < 0.5$ ,  $p_T > 0.15$  GeV/c. Correlation functions in longitudinal co-moving system (LCMS) frame were fitted in low relative momenta region  $|q| < 0.15$  GeV/c via the three-dimensional Gaussian function:

$$C(k_T, q) = 1 + \lambda \exp \left[ -q_{\text{out}}^2 R_{\text{out}}^2 - q_{\text{side}}^2 R_{\text{side}}^2 - q_{\text{long}}^2 R_{\text{long}}^2 \right], \quad (35)$$

where we use standard Bertsch-Pratt notation for

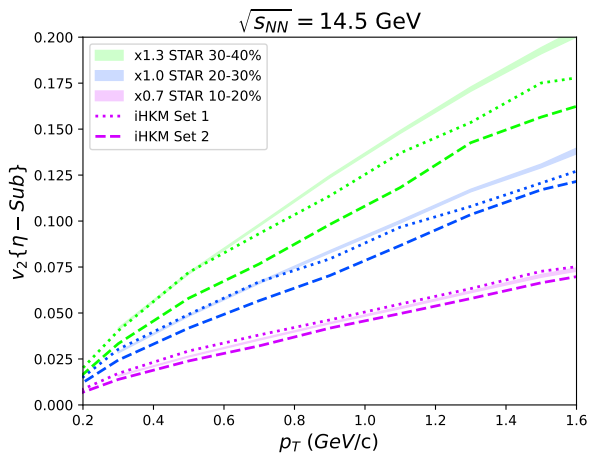


FIG. 3. Elliptic flow coefficients  $v_2$  depends on transverse momenta based on  $\eta$ -subtraction method. The experimental data is taken from [50]. The dashed region accounts for statistical error. Additional multipliers were added to visually separate plots from different centrality classes. Parameters of iHKM are described in Table I.

*out-side-long* coordinate system [53, 54]. Resulting  $R_{out,side,ling}$  dependencies on  $k_T$  presented on Fig. 4. Since experimental data for pion femtoscopy at 14.5 GeV has not been published yet, we present experimental data for two neighboring energies 11.5 GeV and 19.6 GeV [51], assuming that expected values must fall between them.

As one might see in Fig. 4, similarly to elliptic flow  $v_2$  results, iHKM performs much better if the equation of state with crossover type transition is used. A large overestimate of  $R_{long}$  in model calculations with Set 2, can be related to a relatively long hydrodynamic stage compared to the Set 1 scenario. This is resulted both by peculiarities of softer (lower pressure) EoS at low temperatures and later transition to the hadron stage due to the lower  $\epsilon_{sw}$ .

#### D. Maximal emission times estimate

Recently a simple method for the extraction of the times of maximal emission for kaons and pions using the combined fitting of their transverse momentum spectra and the longitudinal interferometry radii dependencies on the pair transverse momentum  $k_T$  has been developed [55]. For the details we address the reader to our previous papers where this method was applied for ultrarelativistic heavy-ion collisions [14, 56, 57]. Here we present only the final expressions for analytical fits:

$$R_{long}^2(k_T) = \tau^2 \lambda^2 \left( 1 + \frac{3}{2} \lambda^2 \right), \quad (36)$$

$$p_0 \frac{d^3 N}{dp^3} \propto \exp \left( - (m_T/T + \alpha) (1 - \bar{v}_T^2)^{1/2} \right), \quad (37)$$

where  $T$  is the effective temperature of the freeze-out hypersurface,  $m_T$  is the transverse mass of particle pair in the LCMS system, while

$$\bar{v}_T = \frac{k_T}{m_T + \alpha T} \quad (38)$$

is the transverse collective velocity at the saddle point. The  $\alpha$  parameter, which is different for pions and kaons, characterizes the intensity of collective transverse flow<sup>1</sup>, while  $\lambda$  is defined via the homogeneity length in the longitudinal direction in the presence of transverse flow

$$\lambda^2 = \frac{\lambda_{long}^2}{\tau^2} = \frac{T}{m_T} (1 - \bar{v}^2)^{1/2}. \quad (39)$$

Using Eqs. (36) and (37), we estimated the maximal emission time  $\tau$  of pions and kaons in 5% of the most central collision. First, we extract the effective temperature from the simultaneous fit of pion and kaon transverse momentum spectra via Eq. (37), which yields  $T = 141 \pm 4.5$  GeV. Then, the other parameters were extracted from the  $R_{long}(m_T)$  dependence using Eq. (36) for both scenarios considered in the paper. The obtained results are demonstrated in Table. II and Fig. 5.

In both cases (Set 1 or Set 2), pions are emitted slightly earlier than kaons, in agreement with our previous findings for ultrarelativistic energies. This observation could be explained by intense processes of  $K^*(892)$  decay during the afterburn stage.

Also, observe that the fit reflects a higher influence of the flow on kaon emission than pions (smaller values of  $\alpha$ ), leading to  $k_T$  or  $m_T$  scaling at large momenta.

Finally, as mentioned in the previous section, our calculations with different equations of state result in different lifetimes of the system while reproducing the momentum spectra. That result aligns well with the overall longer lifetime of the system in the case of a softer equation of state (Set 2) leading to the larger lengths of homogeneity in *long* and *out* directions, as shown in Fig. 4.

TABLE II. Parameters obtained from the fit of transverse momentum spectra and HBT interferometry in iHKM simulations for Au+Au collisions at  $\sqrt{s_{NN}} = 14.5$  GeV. The temperature  $T$  in both fits is  $141 \pm 4.5$  MeV.

| Title | $\alpha_\pi$    | $\alpha_K$      | $\tau_\pi$ (fm/c) | $\tau_K$ (fm/c) |
|-------|-----------------|-----------------|-------------------|-----------------|
| set 1 | $1.74 \pm 0.26$ | $0.24 \pm 0.22$ | $6.59 \pm 0.13$   | $7.74 \pm 0.21$ |
| set 2 | $1.82 \pm 0.36$ | $0.07 \pm 0.06$ | $7.57 \pm 0.19$   | $9.18 \pm 0.18$ |

<sup>1</sup> Infinite  $\alpha$  corresponds to the absence of flow, while small  $\alpha$  values mean strong flow.

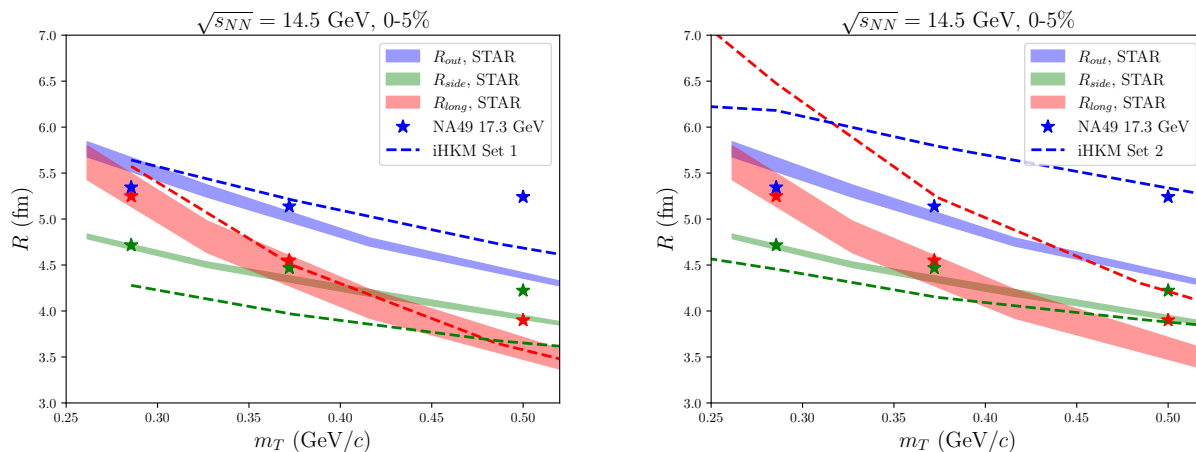


FIG. 4. iHKM results for the  $m_T$  dependence of  $R_{out}$ ,  $R_{side}$  and  $R_{long}$  for negatively charged pions in 5% the most central collisions of gold nuclei at  $\sqrt{s_{NN}} = 14.5$  GeV. Left: iHKM results with crossover transition, and right: with first-order phase transition. Shaded regions cover values between STAR measurements for 11.5 GeV and 19.6 GeV [51]. Additionally, experimental results from the NA49 collaboration for Pb+Pb collisions at 17.3 GeV [52] are included for reference.

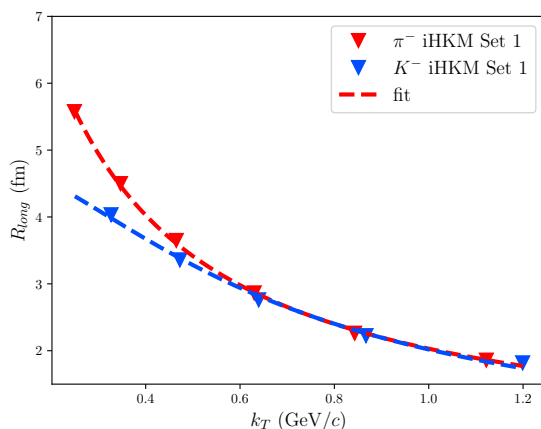


FIG. 5. Two-pion and two-kaon  $R_{long}(k_T)$  dependence obtained from iHKM simulation with two different sets of parameters (see Table I).

#### IV. SUMMARY

In this work, we extend the previously developed integrated hydrokinetic model (iHKM), originally designed to describe soft physics in ultra-relativistic nucleus-nucleus collisions at top RHIC and LHC energies, to a different category of nucleus-nucleus collision experiments characterized by high central net baryon densities. Namely, those carried out at intermediate and low relativistic energies in the current BES RHIC, HADES GSI, and future CBM FAIR experiments. In both ultrarelativistic and semirelativistic cases, we are dealing with the stage of the initial formation of a state (quark-gluon or nucleon) that begins just after overlapping the wave

packets of colliding nuclei. The possible thermalization (full or partial, depending on the collision energy) of the formed matter, and subsequent stages of the evolution of such a matter are investigated. The most striking difference between the mentioned collision energy intervals is based on the time scales of collision processes. The simple estimates of the ratio of the overlapping times of wave packets at the energies per colliding nucleon pair at 5.02 TeV vs. at 7.7 GeV is about  $10^{-3}$ . Accordingly, the nature of the initial pre-thermal collision processes changes dramatically, particularly the time onset of thermalization of the matter evolution and its duration. These values at the energies like at BES RHIC are significantly higher than in the case of ultrarelativistic collisions.

Summarizing, a model has been developed to describe the soft physics processes at the relativistic energies 2–50 GeV per nucleon pair. A radical modification compared to the well-known iHKM model is the simulation of the initial stage of collisions at (relatively) low energy in the quasi-classical UrQMD model instead of the CGC+GLISSANDO representation for ultra-relativistic collisions. In addition to the basic theoretical foundations of the model, we also gave examples describing within its framework the spectra of pions, kaons, protons, and antiprotons for the intermediate energy of 14.5 GeV. Publications have also been prepared to describe the spectra, elliptical fluxes, and femtoscopy radii of the mentioned particles in the energy region from 7.7 to 39 GeV/nuclear pair, describing the data and aiming to investigate the possible phase transition interval.

#### ACKNOWLEDGMENTS

The authors thank O.Vityuk and V.Naboka for their initial scientific contribution to this topic. Also, the au-

thors acknowledge N. Rathod and H. Zbroszczyk for their support, and the work under the further important con-

tribution to the developed model. This work was also supported by a grant from the Simons Foundation (Grant No. 1290596, M.A.).

- 
- [1] J. Rafelski, Connecting QGP-Heavy Ion Physics to the Early Universe, *Nucl. Phys. B Proc. Suppl.* **243-244**, 155 (2013), arXiv:1306.2471 [astro-ph.CO].
- [2] J. Adams *et al.* (STAR), Experimental and theoretical challenges in the search for the quark gluon plasma: The STAR Collaboration’s critical assessment of the evidence from RHIC collisions, *Nucl. Phys. A* **757**, 102 (2005), arXiv:nucl-ex/0501009.
- [3] K. Adcox *et al.* (PHENIX), Formation of dense partonic matter in relativistic nucleus-nucleus collisions at RHIC: Experimental evaluation by the PHENIX collaboration, *Nucl. Phys. A* **757**, 184 (2005), arXiv:nucl-ex/0410003.
- [4] B. B. Back *et al.* (PHOBOS), The PHOBOS perspective on discoveries at RHIC, *Nucl. Phys. A* **757**, 28 (2005), arXiv:nucl-ex/0410022.
- [5] I. Arsene *et al.* (BRAHMS), Quark gluon plasma and color glass condensate at RHIC? The Perspective from the BRAHMS experiment, *Nucl. Phys. A* **757**, 1 (2005), arXiv:nucl-ex/0410020.
- [6] J. A. Wheeler, On the Mathematical Description of Light Nuclei by the Method of Resonating Group Structure, *Phys. Rev.* **52**, 1107–1122 (1937) **52**, 1107 (1937).
- [7] P. D. B. Collins, *An Introduction to Regge Theory and High Energy Physics*, Cambridge Monographs on Mathematical Physics (Cambridge University Press, 2023).
- [8] V. Barone and E. Predazzi, *High-Energy Particle Diffraction*, Texts and Monographs in Physics, Vol. v.565 (Springer-Verlag, Berlin Heidelberg, 2002).
- [9] L. D. Landau, On the multiparticle production in high-energy collisions, *Izv. Akad. Nauk Ser. Fiz.* **17**, 51 (1953).
- [10] J. D. Bjorken, Highly Relativistic Nucleus-Nucleus Collisions: The Central Rapidity Region, *Phys. Rev. D* **27**, 140 (1983).
- [11] M. Borysova and Y. Sinyukov, Hydrodynamic source with continuous emission in Au+Au collisions at 200 GeV, *Phys. Rev. C* **73**, 024903 (2006), arXiv:0507.057 [nucl-th].
- [12] V. M. Shapoval, M. D. Adzhymambetov, and Y. M. Sinyukov, Femtoscopy scales and particle production in the relativistic heavy ion collisions from Au+Au at 200 AGeV to Xe+Xe at 5.44 ATeV within the integrated hydrokinetic model, *Eur. Phys. J. A* **56**, 56260 (2020).
- [13] V. Y. Naboka, S. V. Akkelin, I. A. Karpenko, and Y. M. Sinyukov, Initialization of hydrodynamics in relativistic heavy ion collisions with an energy-momentum transport model, *Phys. Rev. C* **91**, 014906 (2015), arXiv:1411.4490 [nucl-th].
- [14] V. M. Shapoval, M. D. Adzhymambetov, and Y. M. Sinyukov, Femtoscopy scales and particle production in the relativistic heavy ion collisions from Au+Au at 200 AGeV to Xe+Xe at 5.44 ATeV within the integrated hydrokinetic model, *Eur. Phys. J. A* **56**, 260 (2020), arXiv:2006.16697 [nucl-th].
- [15] J. N. Guenther, Overview of the QCD phase diagram: Recent progress from the lattice, *Eur. Phys. J. A* **57**, 136 (2021), arXiv:2010.15503 [hep-lat].
- [16] V. Y. Naboka, I. A. Karpenko, and Y. M. Sinyukov, Thermalization, evolution, and observables at energies available at the CERN Large Hadron Collider in an integrated hydrokinetic model of A+A collisions, *Phys. Rev. C* **93**, 024902 (2016), arXiv:1508.07204 [hep-ph].
- [17] O. Aharony, S. S. Gubser, J. M. Maldacena, H. Ooguri, and Y. Oz, Large N field theories, string theory and gravity, *Phys. Rept.* **323**, 183 (2000), arXiv:hep-th/9905111.
- [18] J. M. Maldacena, TASI 2003 lectures on AdS / CFT, in *Theoretical Advanced Study Institute in Elementary Particle Physics (TASI 2003): Recent Trends in String Theory* (2003) pp. 155–203, arXiv:hep-th/0309246.
- [19] J. Maldacena, The Gauge/gravity duality, in *Black holes in higher dimensions*, edited by G. T. Horowitz (2012) pp. 325–347, arXiv:1106.6073 [hep-th].
- [20] J. Casalderrey-Solana, H. Liu, D. Mateos, K. Rajagopal, and U. A. Wiedemann, *Gauge/String Duality, Hot QCD and Heavy Ion Collisions* (Cambridge University Press, 2014) arXiv:1101.0618 [hep-th].
- [21] A. Bernamonti and R. Peschanski, Time-dependent AdS/CFT correspondence and the Quark-Gluon plasma, *Nucl. Phys. B Proc. Suppl.* **216**, 94 (2011), arXiv:1102.0725 [hep-th].
- [22] O. DeWolfe, S. S. Gubser, C. Rosen, and D. Teaney, Heavy ions and string theory, *Prog. Part. Nucl. Phys.* **75**, 86 (2014), arXiv:1304.7794 [hep-th].
- [23] W. G. Unruh, Notes on black hole evaporation, *Phys. Rev. D* **14**, 870 (1976).
- [24] L. C. B. Crispino, A. Higuchi, and G. E. A. Matsas, The Unruh effect and its applications, *Rev. Mod. Phys.* **80**, 787 (2008), arXiv:0710.5373 [gr-qc].
- [25] Y. Sinyukov, A. N. Nazarenko, and I. A. Karpenko, Is early thermalization really needed in A+A collisions?, *Acta Phys. Polon. B* **40**, 1109 (2009), arXiv:0901.3922 [nucl-th].
- [26] M. Rybczynski, G. Stefanek, W. Broniowski, and P. Bozek, GLISSANDO 2 : GLauber Initial-State Simulation AND mOre... , ver. 2, *Comput. Phys. Commun.* **185**, 1759 (2014), arXiv:1310.5475 [nucl-th].
- [27] M. Bleicher *et al.*, Relativistic hadron hadron collisions in the ultrarelativistic quantum molecular dynamics model, *J. Phys. G* **25**, 1859 (1999), arXiv:hep-ph/9909407.
- [28] H. Petersen, D. Oliinychenko, M. Mayer, J. Staudenmaier, and S. Ryu, SMASH – A new hadronic transport approach, *Nucl. Phys. A* **982**, 399 (2019), arXiv:1808.06832 [nucl-th].
- [29] S. Akkelin, P. Braun-Munzinger, and Y. Sinyukov, Reconstruction of hadronization stage in Pb +Pb collisions at 158 AGeV/c, *Nuclear Physics A* **710**, 439 (2002).
- [30] D. Oliinychenko and H. Petersen, Deviations of the Energy-Momentum Tensor from Equilibrium in the Initial State for Hydrodynamics from Transport Approaches (2016), arXiv:1508.04378 [nucl-th].
- [31] H. Petersen, J. Steinheimer, G. Burau, M. Bleicher, and H. Stöcker, A Fully Integrated Transport Approach to Heavy Ion Reactions with an Intermediate

- Hydrodynamic Stage, Phys. Rev. C **78**, 044901 (2008), arXiv:0806.1695 [nucl-th].
- [32] S. V. Akkelin and Y. M. Sinyukov, Matching of nonthermal initial conditions and hydrodynamic stage in ultrarelativistic heavy-ion collisions, Phys. Rev. C **81**, 064901 (2010), arXiv:0912.4180 [nucl-th].
- [33] W. Israel and J. M. Stewart, Transient relativistic thermodynamics and kinetic theory, Annals Phys. **118**, 341 (1979).
- [34] I. Karpenko, P. Huovinen, and M. Bleicher, A 3+1 dimensional viscous hydrodynamic code for relativistic heavy ion collisions, Comput. Phys. Commun. **185**, 3016 (2014), arXiv:1312.4160 [nucl-th].
- [35] J. Steinheimer, S. Schramm, and H. Stoecker, An Effective chiral Hadron-Quark Equation of State, J. Phys. G **38**, 035001 (2011), arXiv:1009.5239 [hep-ph].
- [36] P. F. Kolb and U. W. Heinz, Hydrodynamic description of ultrarelativistic heavy ion collisions, preprint (2003), arXiv:nucl-th/0305084.
- [37] P. Huovinen and H. Petersen, Particlization in hybrid models, Eur. Phys. J. A **48**, 171 (2012), arXiv:1206.3371 [nucl-th].
- [38] D. Molnar and Z. Wolff, Self-consistent conversion of a viscous fluid to particles, Phys. Rev. C **95**, 024903 (2017), arXiv:1404.7850 [nucl-th].
- [39] F. Cooper and G. Frye, Comment on the Single Particle Distribution in the Hydrodynamic and Statistical Thermodynamic Models of Multiparticle Production, Phys. Rev. D **10**, 186 (1974).
- [40] H. Grad, On the kinetic theory of rarefied gases, Commun. Pure Appl. Math. **2**, 331 (1949).
- [41] I. A. Karpenko, P. Huovinen, H. Petersen, and M. Bleicher, Estimation of the shear viscosity at finite net-baryon density from  $A + A$  collision data at  $\sqrt{s_{NN}} = 7.7 - 200$  GeV, Phys. Rev. C **91**, 064901 (2015), arXiv:1502.01978 [nucl-th].
- [42] Y. Sinyukov, Direct conversion of mixed phase into free hadronic gas and transverse pion momenta in ultrarelativistic nuclear collisions, Zeitschrift für Physik C **43**, 401–409 (1989).
- [43] N. S. Amelin, R. Lednicky, T. A. Pocheptsov, I. P. Lokhtin, L. V. Malinina, A. M. Snigirev, I. A. Karpenko, and Y. M. Sinyukov, A Fast hadron freeze-out generator, Phys. Rev. C **74**, 064901 (2006), arXiv:nucl-th/0608057.
- [44] H. Holopainen, H. Niemi, and K. J. Eskola, Event-by-event hydrodynamics and elliptic flow from fluctuating initial state, Phys. Rev. C **83**, 034901 (2011), arXiv:1007.0368 [hep-ph].
- [45] A. Schäfer, I. Karpenko, X.-Y. Wu, J. Hammelmann, and H. Elfner (SMASH), Particle production in a hybrid approach for a beam energy scan of Au+Au/Pb+Pb collisions between  $\sqrt{s_{NN}} = 4.3$  GeV and  $\sqrt{s_{NN}} = 200.0$  GeV, Eur. Phys. J. A **58**, 230 (2022), arXiv:2112.08724 [hep-ph].
- [46] J. Cimerman, I. Karpenko, B. Tomasik, and P. Huovinen, Next-generation multifluid hydrodynamic model for nuclear collisions at  $s_{NN}$  from a few GeV to a hundred GeV, Phys. Rev. C **107**, 044902 (2023), arXiv:2301.11894 [nucl-th].
- [47] D. Oliinychenko, A. Sorensen, V. Koch, and L. McLerran, Sensitivity of Au+Au collisions to the symmetric nuclear matter equation of state at 2–5 nuclear saturation densities, Phys. Rev. C **108**, 034908 (2023), arXiv:2208.11996 [nucl-th].
- [48] H. Wolter *et al.* (TMEP), Transport model comparison studies of intermediate-energy heavy-ion collisions, Prog. Part. Nucl. Phys. **125**, 103962 (2022), arXiv:2202.06672 [nucl-th].
- [49] P. Kovtun, D. T. Son, and A. O. Starinets, Viscosity in strongly interacting quantum field theories from black hole physics, Phys. Rev. Lett. **94**, 111601 (2005), arXiv:hep-th/0405231.
- [50] J. Adam *et al.* (STAR), Bulk properties of the system formed in  $Au + Au$  collisions at  $\sqrt{s_{NN}} = 14.5$  GeV at the BNL STAR detector, Phys. Rev. C **101**, 024905 (2020), arXiv:1908.03585 [nucl-ex].
- [51] L. Adamczyk *et al.* (STAR), Beam-energy-dependent two-pion interferometry and the freeze-out eccentricity of pions measured in heavy ion collisions at the STAR detector, Phys. Rev. C **92**, 014904 (2015), arXiv:1403.4972 [nucl-ex].
- [52] D. Das, HBT radii: Comparative studies on collision systems and beam energies, Adv. High Energy Phys. **2018**, 3794242 (2018), arXiv:1807.03605 [nucl-ex].
- [53] G. Bertsch, M. Gong, and M. Tohyama, Pion Interferometry in Ultrarelativistic Heavy Ion Collisions, Phys. Rev. C **37**, 1896 (1988).
- [54] S. Pratt, Pion Interferometry of Quark-Gluon Plasma, Phys. Rev. D **33**, 1314 (1986).
- [55] S. V. Akkelin and Y. M. Sinyukov, The HBT interferometry of expanding sources, Phys. Lett. B **356**, 525 (1995).
- [56] Y. M. Sinyukov, V. M. Shapoval, and V. Y. Naboka, On  $m_T$  dependence of femtoscopy scales for meson and baryon pairs, Nucl. Phys. A **946**, 227 (2016), arXiv:1508.01812 [hep-ph].
- [57] V. M. Shapoval and Y. M. Sinyukov, Kaon and pion maximal emission times extraction from the femtoscopy analysis of 5.02A TeV LHC collisions within the integrated hydrokinetic model, Nucl. Phys. A **1016**, 122322 (2021), arXiv:2107.13089 [nucl-th].